Earth's Future

RESEARCH ARTICLE
10.1029/2022EF003079

Phase Shifts of the PDO and AMO Alter the Translation Distance of Global Tropical Cyclones

Licheng Wang[1], Xihui Gu[1,2,3,4,5,6], Louise J. Slater[6], Jianfeng Li[7], Dongdong Kong[1,3], Xiang Zhang[8], and Jianyu Liu[9]

[1]Department of Atmospheric Science, School of Environmental Studies, China University of Geosciences, Wuhan, China, [2]SongShan Laboratory, Zhengzhou, China, [3]Centre for Severe Weather and Climate and Hydro-Geological Hazards, Wuhan, China, [4]Hubei Key Laboratory of Yangtze Catchment Environmental Aquatic Science, School of Environmental Studies, China University of Geosciences, Wuhan, China, [5]State Environmental Protection Key Laboratory of Source Apportionment and Control of Aquatic Pollution, Ministry of Ecology and Environment, Beijing, China, [6]School of Geography and the Environment, University of Oxford, Oxford, UK, [7]Department of Geography, Hong Kong Baptist University, Hong Kong, China, [8]National Engineering Research Center of Geographic Information System, School of Geography and Information Engineering, China University of Geosciences, Wuhan, China, [9]Hubei Key Laboratory of Critical Zone Evolution, School of Geography and Information Engineering, China University of Geosciences, Wuhan, China

Abstract Recent decadal changes in tropical cyclone (TC) frequency since the mid-1990s have been widely reported; however, it is unclear whether there have also been any changes in TC translation distance. Here, we show that long-term decrease in global TC translation distance during 1975–2020 is caused by an abrupt change point around the year 1997. This change point marks a switch between an increasing translation distance during 1975–1997 and decreasing translation distance during 1998–2020. The shift in TC translation distance is attributed to changes in the distance between the location of TC genesis and land, and the percentage of landfalling TCs to all TCs, which is driven by the Pacific Decadal Oscillation (PDO) and Atlantic Multidecadal Oscillation (AMO) phase switch in the mid-1990s. In the last 20 years, the cool, La Niña-like sea surface temperatures (SST) during the PDO negative phase and the warm SST pattern during the AMO positive phase have enhanced the genesis potential index and the potential intensity in offshore areas, resulting in greater TC genesis landward. Phase shifts of PDO and AMO modulate environmental conditions, regulating TC genesis location and landfall frequency, and their combined effects on the translation distance of Pacific TCs. The warm SST anomalies during the AMO positive phase enhance these circulation patterns in two possible ways: via the Indian Ocean and the subtropical eastern Pacific relaying effects at a multidecadal timescale. Our findings suggest that the PDO and AMO act as key pacemakers for decadal changes in global TC translation distance.

Plain Language Summary Translation distance of tropical cyclones (TCs) directly determines the spatial scope of TC-related damages. Over 1975–2020, global TC translation distance shows long-term decreasing trends which are caused by an abrupt change point around the year 1997. This abrupt change point shifts global TC translation distance from increasing trends to decreasing trends. This shift is directly attributed to changes in the genesis-to-land distance and the landfall frequency of TCs, which is tied to the large-scale modes of climate variability that affect atmospheric circulation over decadal timescales, that is, Pacific Decadal Oscillation (PDO) and Atlantic Multidecadal Oscillation (AMO) phase switch in the mid-1990s. Both local sea surface temperature (SST) anomalies and changes in environmental conditions associated with the regime shifts of the PDO and AMO are favorable for TC genesis landward, especially for the western North Pacific (WNP) TCs strongly affected by both the PDO and AMO. Warm SST anomalies during the AMO positive phase may have two pathways altering the circulation patterns over the WNP induced by the PDO phase shift, thus enhancing the genesis of landward and landfalling TCs in the WNP. Our results suggest that the PDO and AMO have important implications for decadal predictions of global TC translation distance.

Key Points:

- Recent decades have witnessed an abrupt, step-like decrease in the translation distance of global tropical cyclones (TCs)
- This step-like decrease of TC translation distance is significantly related to phase shifts of the Pacific Decadal Oscillation (PDO) and Atlantic Multidecadal Oscillation (AMO)
- Sea surface temperatures anomalies and environmental changes associated with the PDO and AMO phase shifts are consistent with decrease in TC translation distance

Supporting Information:

Supporting Information may be found in the online version of this article.

Correspondence to:

X. Gu and J. Liu,
guxh@cug.edu.cn;
liujy@cug.edu.cn

Citation:

Wang, L., Gu, X., Slater, L. J., Li, J., Kong, D., Zhang, X., & Liu, J. (2023). Phase shifts of the PDO and AMO alter the translation distance of global tropical cyclones. *Earth's Future*, *11*, e2022EF003079. https://doi.org/10.1029/2022EF003079

Received 23 JUL 2022
Accepted 9 FEB 2023

Author Contributions:

Conceptualization: Xihui Gu, Jianyu Liu
Formal analysis: Licheng Wang, Xihui Gu, Jianyu Liu
Funding acquisition: Xihui Gu
Methodology: Licheng Wang, Xihui Gu
Software: Licheng Wang
Supervision: Xihui Gu

1. Introduction

Understanding changes in global tropical cyclone (TC) motions such as translation speed, duration, and migration of TC tracks, has become a topic of considerable interest (Kerry, 2020; Kossin, 2018; L. Li & Chakraborty, 2020; Murakami et al., 2020; Studholme et al., 2022; S. S. Wang & Toumi, 2021), because these TC motions impact the location and extent of storm-related damages (Cui et al., 2020; Lai et al., 2020, 2021; Scoccimarro et al., 2020; L.

Visualization: Licheng Wang
Writing – original draft: Licheng Wang, Xihui Gu
Writing – review & editing: Xihui Gu, Louise J. Slater, Jianfeng Li, Dongdong Kong, Xiang Zhang, Jianyu Liu

Wang et al., 2020; Wei et al., 2021; Q. Zhang et al., 2017, 2018). Observed changes in TC motions during the past several decades include the slowdown in the translation speed of global TCs during 1949–2016 (Kossin, 2018), the increased duration of TCs over China during 1975–2009 (X. Chen et al., 2011), and the migration of global TCs toward coastal areas during 1982–2018 (S. S. Wang & Toumi, 2021). All these changes ultimately affect TC translation distance, which determines the spatial scope of TC-related damages (J. Chen et al., 2021; Czajkowski et al., 2013; Villarini et al., 2014). For example, Hurricane Ike in 2008 developed in the Mid-Atlantic, traveled a long distance (i.e., 7,121 km; above the 87th percentile of translation distances measured in all 391 hurricanes during 1961–2020 over the North Atlantic [NA]) across the central United States, and triggered widespread major flooding in inland states such as Iowa, Illinois, and Missouri (Villarini et al., 2014). Hurricane Sally in 2020, a slow-moving storm with a short translation distance (2,004 km; below the 14th percentile), almost stalled in the US Gulf coast and severely battered the two coastal states of Florida and Alabama, resulting in the loss of power to 5,50,000 people. Despite these major impacts of translation distance, few studies have focused on TC translation distance (J. Chen et al., 2021; L. Wang et al., 2022) in comparison with translation speed, duration, and migration of TC tracks, and changes in global TC translation distance remain unknown.

Whether these observed changes in TC motions are attributable to anthropogenic climate change or to natural climate variability is still controversial (Chan, 2019; T. Knutson et al., 2010; T. R. Knutson et al., 2020; Lee et al., 2020; Patricola & Wehner, 2018; Pielke et al., 2005). Kossin (2018) reported a long-term decreasing trend in observed TC translation speed during 1949–2016 for the first time, and implied that this slowdown was associated with anthropogenic warming. Climate model simulations confirmed a robust slowing of TC motion during 1951–2010 under the 4-K warming experiment (G. Zhang et al., 2020). L. Li and Chakraborty (2020) found a slowdown in the decay of landfalling hurricane intensity during 1967–2018 and suggested that this slower decay would continue under future warming. In addition to the decrease in TC translation speed and decaying intensity of TCs, an anthropogenic climate change signal was detected in the changes of TC track characteristics (Cao et al., 2021; Murakami, 2022; Murakami et al., 2017, 2020; Sobel et al., 2016). For example, it was found that the spatial pattern of changes in TC frequency during 1980–2018 (i.e., substantial decreases in the South Indian Ocean (SIO) and western North Pacific (WNP) and increases in the NA and eastern North Pacific (ENP)) could not be explained by multidecadal internal variability but instead by external forcings, such as greenhouse gases and aerosols (Murakami et al., 2020). Similarly, decreased (increased) TCs in the Northern (Southern) Hemisphere during 1985–2014 relative to the pre-industrial period 1850–1979 were shown to be driven by anthropogenic aerosol emission (Cao et al., 2021). It was also found that anthropogenic forcing increases TC intensity, such as the likelihood of severe TCs (tropical storms and above) over the Arabian Sea (Murakami et al., 2017).

In contrast, other studies have queried the monotonicity of the long-term trend in TC motions (He et al., 2015; Lanzante, 2019; H. Zhao et al., 2018; J. Zhao et al., 2018), and have attributed observed changes in TC motions to multidecadal internal variability (Dai et al., 2022; S. S. Wang & Toumi, 2021; X. Wang et al., 2015). For instance, it has been suggested that the long-term decrease in TC translation speed was caused by abrupt and step-like changes; and that one of these abrupt change points occurred in 1990s (Lanzante, 2019). This abrupt change around the mid-1990s has also been observed in TC frequency and the migration of TCs toward coasts (He et al., 2015; S. S. Wang & Toumi, 2021; H. Zhao et al., 2018; J. Zhao et al., 2018). Specifically, an abrupt increase (decrease) in TC frequency has occurred over the NA (WNP) since the mid-1990s (He et al., 2015; H. Zhao et al., 2018; J. Zhao et al., 2018); and the mean global TC locations tend to have shifted poleward and westward from 1982 to 1999 to 2000–2018 (S. S. Wang & Toumi, 2021). These studies have attributed these decadal changes in TC activities to multidecadal internal variability, especially the Pacific Decadal Oscillation (PDO) and Atlantic Multidecadal Oscillation (AMO), first because the phase shifts of the PDO (AMO) from positive (negative) to negative (positive) in the mid-1990s (Figure S1 in Supporting Information S1) correspond well with this abrupt change point in TC activities. The atmospheric circulation anomalies driven by the phase shifts of the PDO and/or AMO are responsible for the abrupt changes in TC activity (Sun et al., 2017; W. Zhang et al., 2018; Q. Zhang et al., 2018). For example, the PDO negative phase can strengthen and shift the Walker Circulation westward, resulting in increased (decreased) TC activity in the NA (WNP) (Allen & Kovilakam, 2017; Staten et al., 2018; S. S. Wang & Toumi, 2021; H. Zhao et al., 2019). Similarly, the AMO positive phase can intensify vertical wind shear in the southeastern WNP, resulting in decreased WNP TC frequency (Sun et al., 2017; W. Zhang et al., 2018; Q. Zhang et al., 2018). Although impacts of the PDO and AMO on TC activities have been widely investigated, there is still a gap in understanding how the synchronous phase shifts of the PDO and AMO affect changes in the translation distance of global TCs.

In this study, we therefore address the following questions: (a) Does global TC translation distance show a monotonic trend or step-like change during the past several decades; (b) if the latter, is this step-like change in TC translation distance related to the PDO and AMO phase shifts? (c) If yes, how do PDO and AMO phase shifts synergistically modulate the change in global TC translation distance?

2. Data and Methods

2.1. TC Best Track Data

The recently released global TC best track data, that is, International Best Track Archive for Climate Stewardship version 04 (IBTrACS; Knapp et al., 2010), is used in this study. The TC tracks from multiple organizations are compiled and merged in the IBTrACS data set. We choose the combination of TC tracks from the National Hurricane Center and Joint Typhoon Warming Center to cover the North Indian Ocean (NIO), WNP, ENP, NA, SIO, and South Pacific (SP) (see Figure S2 in Supporting Information S1 for the geographical locations of the six basins), which is consistent with previous studies (Kossin, 2018; Murakami et al., 2020). The IBTrACS data set provides TC intensity (maximum sustained wind speed) and geographic position every 6 hr (i.e., 0, 6, 12, and 18 UTC) during the lifetime of all TCs. Due to the problem of inhomogeneity in TC tracks, particularly for the pre-satellite era (Moon et al., 2019), we only utilize the data set during 1975–2020.

2.2. PDO and AMO Indices

Standardized indices of monthly PDO and AMO are obtained from the National Oceanic and Atmospheric Administration Physical Sciences Laboratory. Monthly standardized values of PDO and AMO are averaged annually and seasonally. The TC season in the Northern Hemisphere is from July to October (JASO), and in the Southern Hemisphere is from December to March (DJFM) (Cao et al., 2021). These annual and seasonal time series of PDO and AMO indices are correlated to annual-mean TC translation distance.

2.3. ERA5 Reanalysis Data

We assess monthly values from the Medium-Range Weather Forecasts fifth generation atmospheric reanalysis data set (ERA5; Hersbach et al., 2020) for these variables: zonal and meridional wind components (units: m/s), sea level pressure (units: Pa), air temperature (units: K), specific humidity (units: kg/kg), relative humidity (units: %), vorticity (units: s^{-1}), and sea surface temperature (SST, units: K). The values of these variables are at the $0.25° \times 0.25°$ spatial resolution during 1975–2020.

Based on these variables, we further calculate the steering flow (units: m/s), vertical wind shear (units: m/s), potential intensity, and genesis potential index (GPI). Steering flow is defined as the pressure-weighted deep-layer wind field between 300 and 850 hPa (Aryal et al., 2018; Franklin et al., 1996). Vertical wind shear is estimated using the wind field between 200 and 850 hPa (Zehr, 2003). Following previous studies (Camargo, Emanuel, & Sobel, 2007, 2007b; Emanuel, 2005, 2007), we estimate potential intensity and GPI using 850-hPa vorticity, 700-hPa relative humidity, SST, outflow layer temperature, and convective available potential energy. Potential intensity is the maximum sustainable intensity of TCs; higher potential intensity provides a better condition to intensify TCs. Potential intensity is used to estimate the GPI which is used to quantitatively evaluate the environmental conditions of TC genesis. Higher GPI indicates more TCs could be produced in general.

2.4. Selection of TC Tracks

According to the Saffir–Simpson scale (Simpson & Riehl, 1981), TCs are defined as tropical depressions, tropical storms (TS), severe TS (STS), typhoons (TY), severe TY (STY), and super TY, when their maximum sustained 10-m wind speed is within 10.8–17.1 m/s, 17.2–24.4 m/s, 24.5–32.6 m/s, 32.7–41.4 m/s, 41.5–50.9 m/s, and greater than 51 m/s, respectively. Due to the issue of severe inhomogeneity in tropical depressions (such as fewer tropical depressions are recorded during the pre-satellite era and larger uncertainty in the intensity of tropical depressions), we first exclude the tropical depressions (i.e., TCs with maximum sustained wind speeds of less than 17.1 m/s) from the TC data sets. For each TC track in the filtered data set, we exclude TC positions if they are recorded as extratropical transition or if their sustained 10-m wind speed is less than 10.8 m/s (i.e., the lowest

sustained 10-m wind speed of a TC). Hereafter, the selected partial tracks (see Figure S2 in Supporting Information S1) are referred to as TC tracks in this study. The generation and termination of TC tracks (i.e., the first and last positions) indicate the TC genesis and demise, respectively. Following these filtering steps, a total of 1,167, 589, 810, 222, 660, and 435 TCs remain for our analysis during 1975–2020 over the WNP, NA, ENP, NIO, SIO, and SP, respectively.

In the IBTrACS data set, the distance to the nearest land, including all continents and any islands larger than 1,400 km^2, is given for each TC position of each TC track (see parameter "DIST2LAND"). If the distance in any positions of a TC track is set as zero (i.e., the parameter "DIST2LAND" = 0), this TC is identified as a landfalling TC. 694, 268, 123, 167, 189, and 147 TCs are identified as landfalling TCs over the WNP, NA, ENP, NIO, SIO, and SP, respectively.

2.5. Calculation of TC Translation Distance

In a TC track, each 6-hr interval between two TC positions is taken as a segment. The length of a segment is estimated along a great circle arc. The lengths of all segments in a TC track are summed as the TC translation distance.

For a segment in a TC track, if either one or both of its two positions are over land (i.e., the parameter "DIST2LAND" is zero), this segment is considered as an over-land segment, otherwise as an over-sea segment (Kossin, 2018; S. S. Wang & Toumi, 2021). We then identify all over-land (over-sea) segments for a TC track, and finally sum the lengths of these segments as the over-land (over-sea) translation distance of the given TC.

3. Results and Discussion

3.1. Changes in TC Translation Distance

Temporal changes in annual-mean translation distance of all and landfalling TCs over the globe, Northern Hemisphere, and Southern Hemisphere during 1975–2020 are shown in Figure 1. Both all and landfalling TCs show significant ($p < 0.05$) decreasing translation distance over the globe at rates of −8.42 km per year and −10.05 km per year using linear trend detection (C. Li et al., 2023; Liu et al., 2021; X. Yu et al., 2022). Decreases are also found in the Northern Hemisphere (−7.74 km per year, $p < 0.1$; −9.51 km per year, $p < 0.1$) and the Southern Hemisphere (−4.17 km per year, $p = 0.4$; −9.65 km per year, $p = 0.2$). However, all these decreases are not monotonous downward trends, but due primarily to an abrupt, step-like change. Using the Pettitt method (Pettitt, 1979), we detect an abrupt change point around the year 1997 ($p < 0.05$) in annual-mean translation distance not only for all and landfalling TCs but also for the globe, Northern Hemisphere, and Southern Hemisphere (Figure 1). The annual-mean translation distance shows significantly increasing trends for all and landfalling TCs over the globe, Northern Hemisphere, and Southern Hemisphere before the abrupt change point (i.e., during 1975–1997), and then exhibits a significant step downwards, with slightly decreasing trends after the abrupt change point (i.e., during 1998–2020; only significant in the Southern Hemisphere). Globally, the average translation distance of all (landfall) TCs during 1975–1997 is 3,161 km (3,187 km), and reduced to 2,812 km (2,780 km) and by 11.8% (12.7%) during 1998–2020. This step downward is mainly responsible for the long-term linear decreasing trend of TC translation distance over the entire period of 1975–2020.

We also check changes in TC translation distance in four latitudinal zones (i.e., 15–30°N, 0–15°N, 0–15°S, and 15–30°S; Figure S3 in Supporting Information S1) and six basins (i.e., NIO, WNP, ENP, NA, SIO, and SP; Figures S4 and S5 in Supporting Information S1). The abrupt change point around the year 1997 is detected in almost all four zones and six basins. Additionally, a downward step in TC translation distance is observed in all four zones and six basins. These results indicate that the observed step-like reduction in the translation distance of global TCs is robust.

A key question is therefore understanding what drives this step-change in TC translation distance around the globe. As stronger TCs usually have longer translation distance (J. Chen et al., 2021), we first explore potential effects of changes in TC intensity on TC translation distance. Figure 2a shows the average translation distance in five TC groups classified by TC intensity, that is, TS, STS, TY, STY, and super TY. As TC intensity increases, the average translation distance becomes evidently larger. Moreover, the average translation distance exhibits a reduction during 1998–2020 relative to 1975–1997 in all five groups of both landfalling and non-landfalling

10.1029/2022EF003079

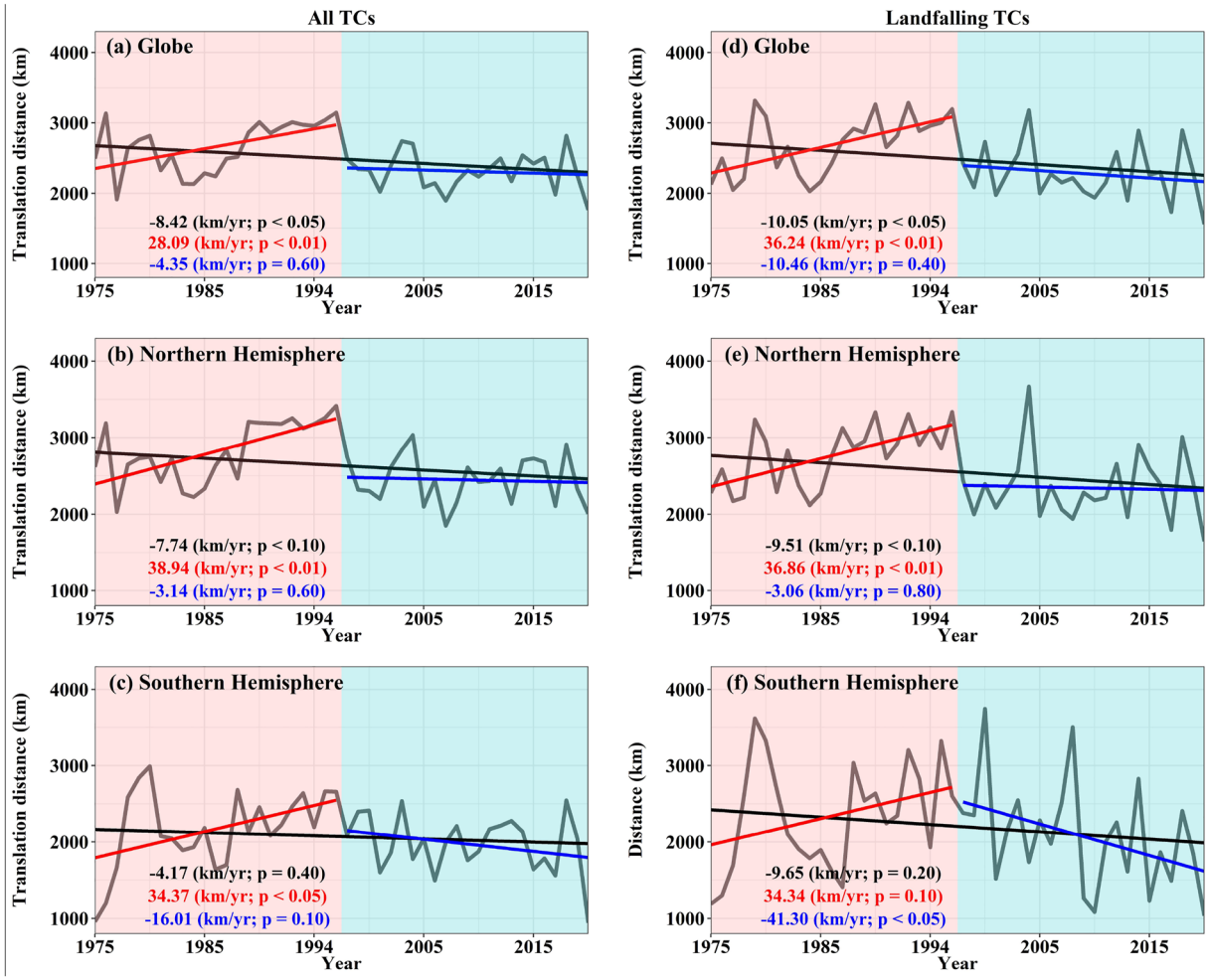

Figure 1. Temporal changes in annual-mean translation distance of tropical cyclones (TCs) over the globe (a and d), the Northern Hemisphere (b and e), and the Southern Hemisphere (c and f) during 1975–2020. The left (right) column is for all (landfalling) TCs. Black, red, and blue lines indicate the linear trends during the whole period (i.e., 1975–2020), before the abrupt change point (i.e., 1975–1997), and after (i.e., 1998–2020), respectively. The abrupt change point is detected around the year 1997 at the 0.05 significance level using the Pettitt method (Pettitt, 1979) and is significant in all 6 panels.

TCs, further confirming the downward TC translation distance shown in Figure 1. We count the percentage of landfalling TS, STS, TY, STY, and super TY during 1975–1997 (1998–2020), as well as non-landfalling TCs (Figure 2b). Although the percentages of TY and STY decrease after the abrupt change point, the proportion of both landfalling and non-landfalling super TY increased during 1998–2020. Previous studies reported that hurricanes are getting stronger due to increasing potential intensity and warming SST (Kerry, 2020; Kossin et al., 2020; Sobel et al., 2016). It is therefore unlikely that the decrease in TC translation distance is driven by changes in TC intensity.

Second, we hypothesize that the decrease in TC translation distance is driven by changes in TC genesis locations. The distance of global TC genesis locations to land has shortened significantly (by −2.13 km per year, $p < 0.05$) during 1975–2020 (Figure 2c). This shortened genesis-to-land distance occurs in both landfalling and non-landfalling TCs (i.e., −2.58 km per year, $p < 0.05$; and −0.84 km per year, $p = 0.4$; Figure 2d). Additionally, this shortening is associated with an abrupt change point around the year 1997 for all, landfalling, and non-landfalling TCs (Figures 2c and 2d). In line with the TC translation distance, the genesis-to-land distance of all, landfalling, and non-landfalling TCs switched from an increasing trend (averages: 913, 696, and 1,053 km) to a decreasing trend (averages: 837, 613, and 1,004 km; i.e., by −8.3%, −11.9%, and −4.7% in the mean genesis-to-land distance) after the abrupt change point.

The landward migration of TC generation is directly determined by its zonal and meridional locations (see Figures S6 and S7 in Supporting Information S1). Further, in all regions except NA, the changepoint favors the poleward

10.1029/2022EF003079

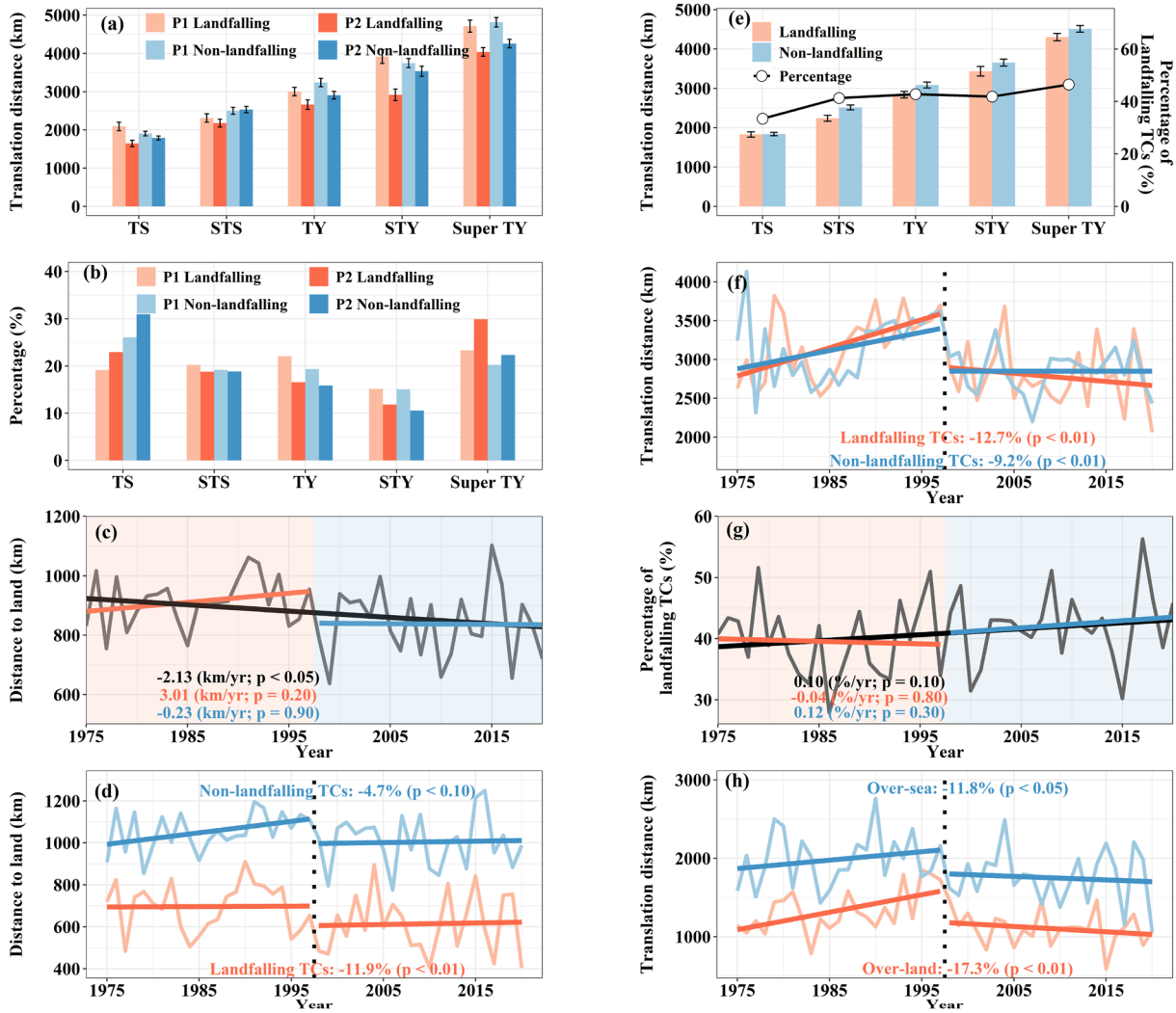

Figure 2. Tropical cyclone (TC) features associated with changes in TC translation distance. In a, average translation distance of landfalling and non-landfalling TCs before and after the abrupt change point, that is, in period 1 (P1, 1975–1997) and period 2 (P2, 1998–2020). Both landfall and non-landfalling TCs are classified into five groups according to TC intensity: tropical storms (TS), severe TS (STS), typhoons (TY), severe TY (STY), and super TY. In (b), percentage (%) of landfalling TCs in each group, TS, STS, TY, STY, and super TY during the P1 (P2) period, as well as non-landfalling TCs. In (c), the distance between each TC generation location and land is averaged annually. The land data set includes all continents and any islands larger than 1,400 km^2. In (d), the same as (c) but for landfalling (red line) and non-landfalling (blue) TCs. In (e), average translation distance of landfalling and non-landfalling TCs classified as TS, STS, TY, STY, and Super TY during 1975–2020. In each group of TC intensity, the percentage of landfalling TCs is also given (see the black line in e). In (f), annual-mean translation distance of landfalling (red line) and non-landfalling (blue lines) TCs. In (g), percentage of landfalling TCs accounting for all TCs in each year. In (h), annual-mean over-land (red line) and over-sea (blue line) translation distance of landfalling TCs, respectively. In (a) and (e), the error bars indicate one standard error.

migration of TC genesis latitudes (Figures S6 and S8 in Supporting Information S1). For annual-mean TC genesis longitude, the abrupt change point interrupts the eastward (westward) trend in the WNP (ENP), and accelerates the westward trend in the NIO and SIO (Figure S7 in Supporting Information S1). These changes in TC genesis longitude and latitude result in a landward movement of TC genesis in the five basins (i.e., WNP, ENP, NIO, SIO, and SP) accounting for 85% of global total TCs during 1975–2020. The closer distance of TC genesis to land shortens TC travel distance over the ocean, and therefore probably also their impact on coastal zones.

Previous studies have a consensus that TC latitudes (including latitudes of TC's lifetime-maximum intensity and genesis) are poleward expansion (Altman et al., 2018; Daloz & Camargo, 2018; Kossin et al., 2014; Shan & Yu, 2020; Sharmila & Walsh, 2018; Studholme et al., 2022). For example, Kossin et al. (2014) reported that the TC's lifetime-maximum intensity in the Northern (Southern) Hemisphere during 1982–2012 is significantly migrated at a rate of 53 (62) km per decade. Daloz and Camargo (2018) further indicated that the poleward

migration of TC's lifetime-maximum intensity is linked to the poleward migration of TC's genesis. The poleward migration of TC latitudes resulted in the migration of TCs toward coasts, considering the geographical relations between TC genesis locations and land (see Figure S2 in Supporting Information S1). For example, the distance of TC's lifetime-maximum intensity to land has significantly decreased by ~30 km per decade globally during 1982–2018 (S. S. Wang & Toumi, 2021). These findings are consistent with the reduced distance of global TC genesis locations to land in our study. Many studies have discussed potential reasons behind the poleward and landward TC locations (Sharmila & Walsh, 2018; Studholme et al., 2022; S. S. Wang & Toumi, 2021). Sharmila and Walsh (2018) linked the poleward shift of TC formations to Hadley cell expansion which is likely to suppress the low-latitude TC generations via anomalous large-scale subsidence. S. S. Wang and Toumi (2021) attributed the landward shift of TC locations to global zonal changes in environmental steering flow. Studholme et al. (2022) indicated that the poleward migration of TCs is likely driven by anthropogenic greenhouse gas emissions.

The distance of TC genesis to land is shortened by 11.9% ($p < 0.01$) for landfalling TCs after the abrupt change point, and this percentage is more than double that (i.e., 4.7%, $p < 0.1$) of non-landfalling TCs (Figure 2d). It seems that this reduction in the distance to land is more obvious in landfalling TCs. Additionally, although the translation distance of both landfalling and non-landfalling TCs switches from increasing trends to decreasing trends in the year 1997, the switch is sharper for landfalling TCs (Figure 2f). Specifically, after the abrupt change point, the translation distance of landfalling (non-landfalling) TCs is shortened by 12.7% (9.2%; both $p < 0.01$).

We therefore hypothesize that changes in landfalling TC frequency may also affect the TC translation distance. After TCs make landfall, TC intensity usually decays rapidly due to terrain blocking effects and lack of moisture from oceans (L. Li & Chakraborty, 2020), resulting in a shorter translation distance than non-landfalling TCs (Figure 2e). There is an increasing trend in the percentage of landfalling to total TCs during 1975–2020 (i.e., 0.10% per year, $p = 0.1$; Figure 2g). The long-term change in the percentage of landfalling TCs also switches from a decreasing trend (−0.04% per year, $p = 0.8$) to an increasing trend (0.12% per year, $p = 0.3$) after the abrupt change point. We further divide the translation distance of landfalling TCs into over-sea and over-land parts. Both over-sea and over-land translation distance of landfalling TCs show consistent behavior with the translation distance of landfalling TCs shown in Figure 1d. Nevertheless, this shift is move obvious over land, and shortens the over-land translation distance by 17.3% ($p < 0.01$; and this value is 11.8% at the 0.05 significance level for the over-sea translation distance).

Overall, as the translation distance of all and landfalling TCs decreases after the 1997 change point, a synchronous shift occurs over the globe, Northern Hemisphere, Southern Hemisphere, and almost all regions (except landfalling TCs over the NIO), that is, from increasing to decreasing trends. This shift is directly associated with the decrease in the distance of global TC genesis locations to land and the increase in the percentage of landfalling TCs.

3.2. Relations Between TC Translation Distance and PDO and AMO

Both natural variability and anthropogenic forcing affect TC activities. The switch in the trends of TC translation distance after the 1997 change point reduces the likelihood that the reduction of TC translation distance is driven primarily by anthropogenic forcing. The opposite trend directions of TC translation distance before and after the change point (two 23-years periods: 1975–1997 and 1998–2020) suggest that the driving regime may be shifting from one mode to another mode at a multidecadal timescale. Given that TC translation distance shows decadal variability and both the PDO and AMO switched their phases around the abrupt change point (i.e., the year 1997; Figure S1 in Supporting Information S1), it is therefore reasonable to postulate that the observed shift in TC translation distance may be linked to the phase shifts of the two climate modes.

To assess this postulate, we estimate Spearman correlations between annual-mean TC translation distance and PDO and AMO indices (Figure 3). With the exception of the NA and SIO, positive (negative) correlations are found between annual-mean translation distance of all and landfalling TCs and PDO (AMO), especially over the Pacific (including WNP, ENP, and SP; almost all correlations at the 0.05 significance level). For the NA, there are weak negative (positive) correlations with PDO (AMO), but boreal TC-season (i.e., JASO) AMO is significantly related to annual-mean TC translation distance over this basin. The pattern of correlations for the SIO is similar to the NA, but only PDO has significantly negative correlations with annual-mean translation distance of landfalling

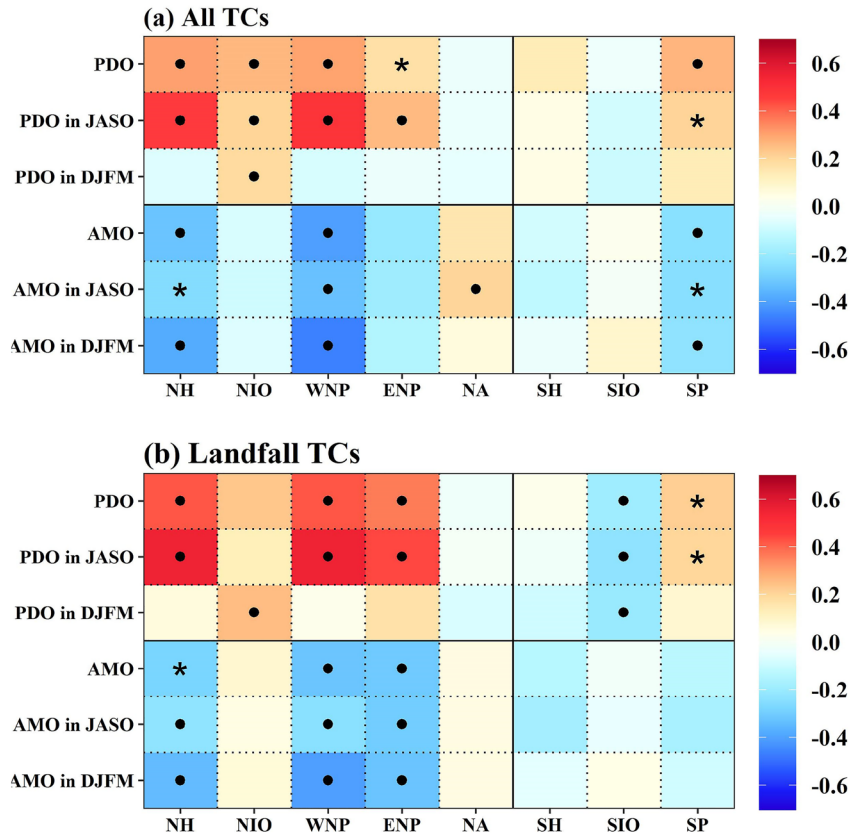

Figure 3. Spearman correlations between annual-mean TC translation distance and Pacific Decadal Oscillation (PDO) or Atlantic Multidecadal Oscillation (AMO) indices. Both monthly PDO and AMO indices are averaged annually and seasonally (i.e., July–October, JASO; and December–March, DJFM). These annual and seasonal PDO and AMO time series are correlated to annual-mean TC translation distance of all (a) and landfalling (b) TCs over the Northern Hemisphere, North Indian Ocean, western North Pacific, eastern North Pacific, North Atlantic, Southern Hemisphere, South Indian Ocean, and South Pacific, respectively. The black dots/asterisks indicate the correlations are significant at the 0.05/0.1 level, respectively.

TCs over the SIO (Figure 3b). The correlations between PDO (AMO) and annual-mean TC translation distance are opposite between over the SIO and SP, possibly resulting in weak correlations between annual-mean translation distance over the Southern Hemisphere and PDO (AMO). Overall, the significant correlations between annual-mean TC translation distance and PDO and AMO indicate that PDO and AMO are likely to be driving the step-like change in translation distance of TCs, specifically over the basins in the Pacific.

To further evaluate this hypothesis, we assess the influence of changes in SST and the environmental patterns associated with the phase shifts of PDO and AMO on the genesis locations and landfall frequency of TCs (mentioned above; see Figure 2). SSTs and environmental patterns are two key factors driving the step-like change in TC translation distance. When the PDO phase switched from positive to negative in the mid-1990s, the pattern of SST anomalies in the tropical Pacific shifted to a La Niña-like state, that is, the subtropical WNP (tropical eastern Pacific) became warmer (cooler) (Figures S9a and S9b in Supporting Information S1). The La Niña-like SST pattern leads to significantly positive (negative) GPI and potential intensity anomalies in the offshore (central) areas of the North Pacific (Figures 4a, 4b, 5a, and 5b), resulting in landward cyclogenesis (see abrupt northwestward and northeastward shift of TC genesis over the WNP and ENP, respectively; Figures S6b, S6c, S7b, and S7c in Supporting Information S1). Given the dependence of TC duration on genesis location in the North Pacific (Scoccimarro et al., 2021), TCs with northward genesis positions tend to show shorter duration. The landward cyclogenesis and shorter TC duration would lead to the reduced translation distance of TCs over the North Pacific (both the WNP and ENP). Previous studies also pointed out that this La Niña-like SST pattern is also responsible for the sudden decrease of TC frequency over the WNP since the mid-1990s (He et al., 2015; Hsu et al., 2014; H. Zhao et al., 2018; J. Zhao et al., 2018). Specifically, more (fewer) TCs are produced in the offshore

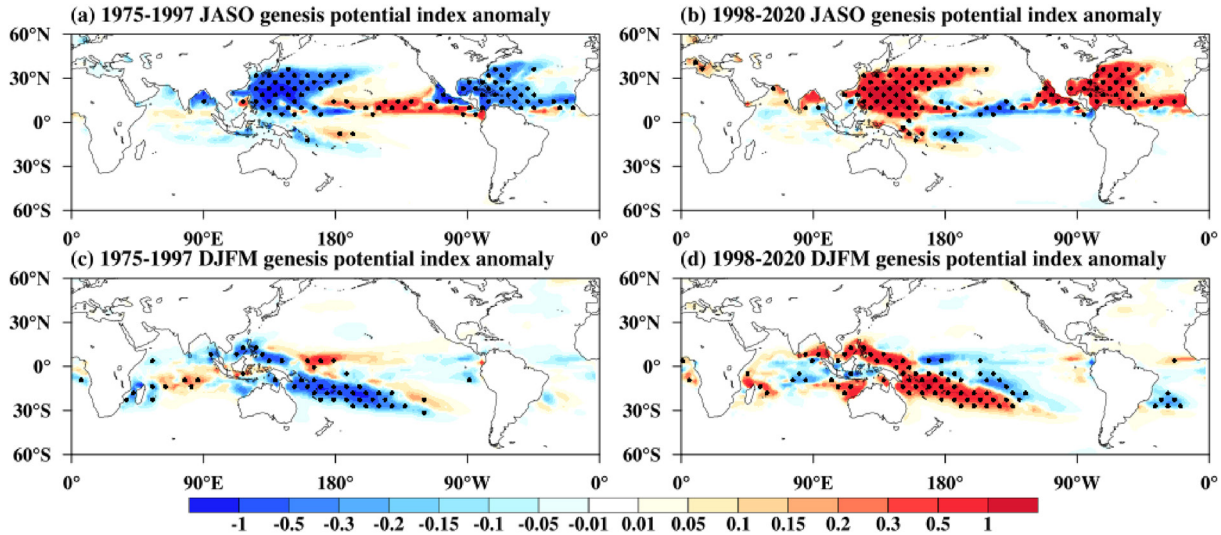

Figure 4. Composited seasonal genesis potential intensity (GPI) anomalies during 1975–1997 (a and c) and 1998–2020 (b and d). The anomalies are computed as the absolute difference of TC-season means between 1975 and 1997 (1998–2020) and the reference period 1981–2010. The TC season is July–October (JASO) in the Northern Hemisphere and December–March (DJFM) in the Southern Hemisphere. The stippling indicates the anomalies are significant at the 0.05 level using the Student's *t* method.

areas of the WNP (the southeast WNP), especially for the recurved TCs (formed in the southeast WNP and recurved along the East Asian coast; these recurved TCs usually have longer translation distance than other TCs over the WNP, i.e., westward ones and northwestward ones; He et al., 2015; Hsu et al., 2014; H. Zhao et al., 2018; J. Zhao et al., 2018). The enhanced TC genesis over the offshore areas of the WNP and suppressed recurved TCs also contribute to the decrease in annual-mean TC translation distance over the WNP since the mid-1990s.

The change in TC genesis over the SP is almost symmetrical to the change in TC genesis over the WNP along the equator. During the PDO negative phase, the southwest SP shows warming SST anomalies (Figures S9c and S9d in Supporting Information S1), accompanied by significantly positive GPI and potential intensity anomalies over the offshore areas (Figures 4c, 4d, 5c, and 5d). This SST pattern is favorable for TC genesis southward (see the sudden increase in annual-mean latitude of TC genesis shown in Figure S6f of the Supporting Information S1), resulting in a shorter cyclogenesis-to-land distance.

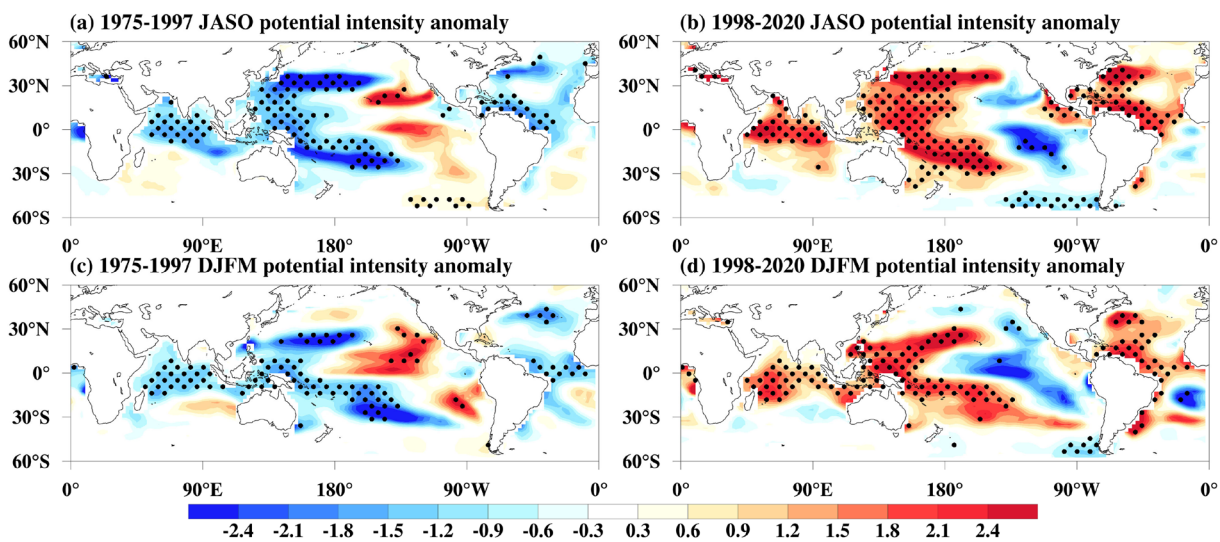

Figure 5. The same as Figure 4, but for potential intensity anomalies during 1975–1997 (a and c) and 1998–2020 (b and d). The stippling indicates the anomalies are significant at the 0.05 level using the Student's *t* method.

10.1029/2022EF003079

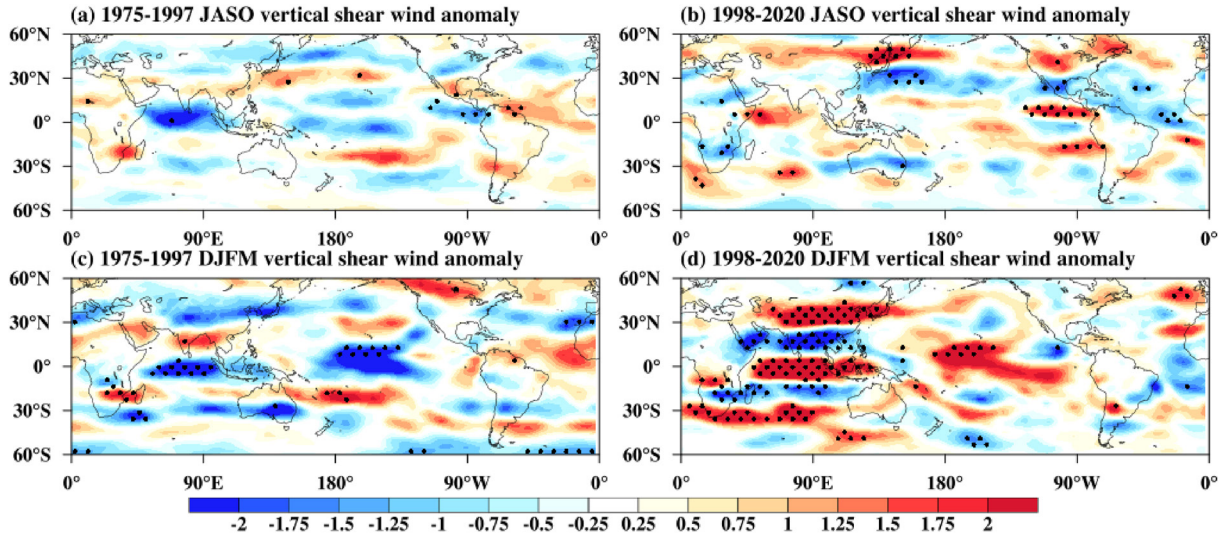

Figure 6. The same as Figure 4, but for vertical wind shear anomalies (units: m/s). The stippling indicates the anomalies are significant at the 0.05 level using the Student's *t* method.

Beside the effects of local SST anomalies, the changes in environmental conditions associated with the PDO and AMO are also consistent with the step-like reduction in translation distance of TCs over the Pacific (Figures 6–8). During PDO negative and AMO positive phases, the areas (the subtropical WNP, ENP offshore areas, and southwest SP) with warmer SST anomalies, enhanced GPI and potential intensity, experience weakened vertical wind shear (Figures 6a and 6b) and increased low-level relative humidity (Figures 7a and 7b), and thus provide favorable thermodynamic and dynamic conditions for TC genesis poleward and landward. In the WNP, anomalous cyclonic (anticyclonic) steering flow over the southwestern (northwestern) areas guides more landfalling TCs toward the East Asia mainland (Figures 8a and 8b; Choi & Kim, 2019; Yong & Chen, 2019). However, the enhanced vertical wind shear and decreased relative humidity over northeast Asia impede the TCs from traveling a long distance over the land. The La Niña-like SST anomalies over the Pacific in the last 20 years have enhanced the Walker circulation in the tropical Pacific and weakened the WNP monsoon trough (Shi et al., 2020), suppressing recurved TCs produced in the southeast WNP (H. Zhao et al., 2018; J. Zhao et al., 2018). An anomalous anticyclonic steering flow over the northwest ENP and prevailing easterlies over the subtropical ENP (Figures 8a

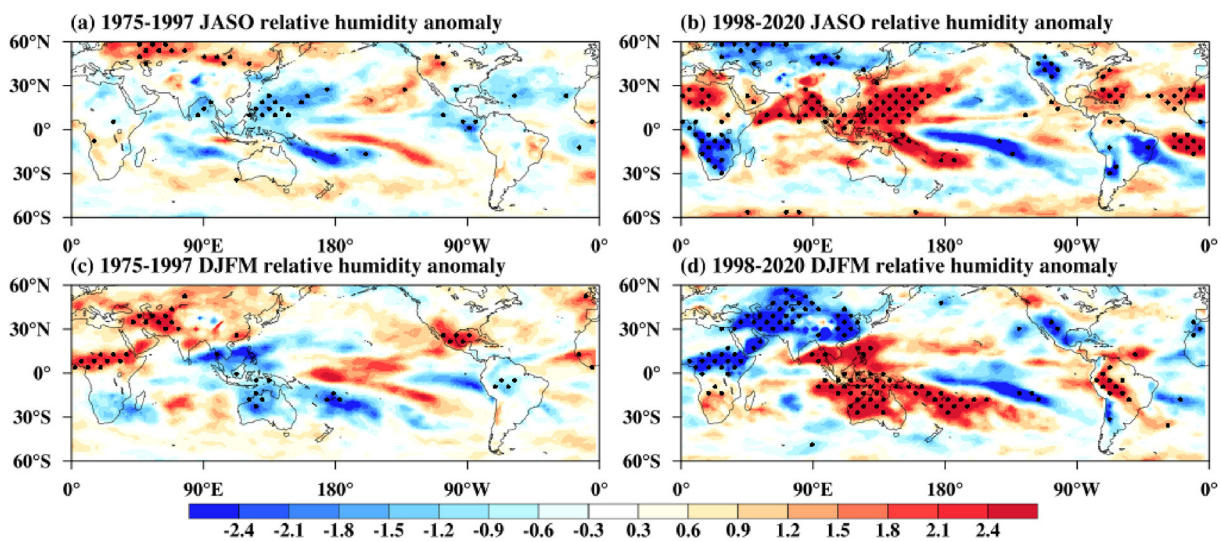

Figure 7. The same as Figure 4, but for 700-hPa relative humidity anomalies (units: %). The stippling indicates the anomalies are significant at the 0.05 level using the Student's *t* method.

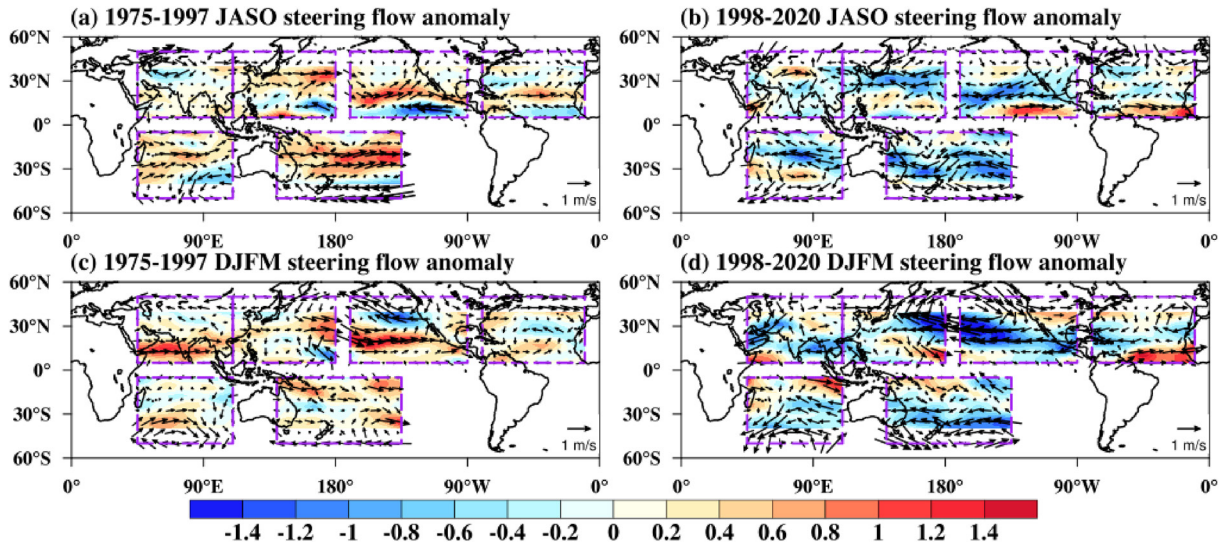

Figure 8. The same as Figure 4, but for steering flow anomalies (vector; units: m/s) and 500-hPa zonal wind anomalies (shading; units: m/s).

and 8b) drive more TCs toward the Central Pacific. The enhanced vertical wind shear, decreased relative humidity, and weakened potential intensity over the central North Pacific partially explain the reduced TC translation distance over the ENP. In the SP, an anomalous cyclonic steering flow over the northwest areas and prevailing easterlies (Figures 8c and 8d) prevent TC movement eastward and promote a greater number of landfalling TCs over Australia, where the enhanced vertical wind shear (Figures 6c and 6d) does not favor the translation of TCs over the land.

Although only the PDO is significantly positively (negatively) correlated to the translation distance of all (landfalling) TCs over the NIO (SIO), both basins show decreases in TC translation distance after the abrupt change point (Figures S4 and S5 in Supporting Information S1). After the abrupt change point, the offshore areas of both NIO and SIO show enhanced GPI and potential intensity (Figures 4 and 5), resulting in landward TC genesis (i.e., northeastward/southeastward for the NIO/SIO, as shown in Figures S6a, S6e, S7a, and S7e of the Supporting Information S1). For the SIO, the belt region crossing Madagascar Island (also the main TC generation region; Figures S9c and S9d in Supporting Information S1) shows weakened vertical wind shear (Figures 6c and 6d) and increased low-level relative humidity (Figures 7c and 7d), which also promotes greater TC genesis eastward. On the other hand, the prevailing easterlies over this belt region (Figures 8c and 8d) hinder the eastward movement of TCs over the SIO, resulting in a reduction TC translation distance in recent two decades. Previous studies have indicated that the Indian Ocean primarily features a basin-wide decadal warming/cooling pattern at an interdecadal timescale, termed the interdecadal Indian Ocean Basin Mode (Cheung et al., 2015; Han et al., 2014; Z. Zhang et al., 2018). These local SST anomalies play a key role in modulating TC trajectories over the NIO and SIO (Cheung et al., 2015), which is beyond our study scope.

Only the AMO is significantly and positively correlated to the translation distance of TCs over the NA (Figure 3a), indicating that the AMO positive phase in the last 20 years has been beneficial for TCs over the NA traveling a long distance. During the AMO positive (negative) phase, warm (cool) SST anomalies are found over the whole NA (Figures S9a and S9b in Supporting Information S1), as well as significantly positive (negative) GPI and potential intensity anomalies (Figures 4a, 4b, 5a, and 5b). This intensified GPI and potential intensity have enhanced basin-scale TC formation over the NA since the mid-1990s (i.e., from 215 to 374 TCs identified in our study, i.e., an increase of 74%), which was also reported in previous studies (R. Wang & Wu, 2013; H. Zhao et al., 2018; J. Zhao et al., 2018). The increase in TC frequency during the AMO positive phase is mainly found over the east tropical Atlantic, far from the North American continent (Holland, 2007; Wu & Wang, 2008; Wu et al., 2010), suggesting that TCs are more likely to travel for a long duration (Wu et al., 2010) and thus have a large translation distance.

Not only the warmer SSTs but also changes in environmental patterns provide favorable conditions for enhanced TC formation in the east tropical Atlantic. Basin-scale increases in 700-hPa relative humidity and weakened

vertical wind shear during the AMO positive phase favor the enhancement of TC formation over the NA, especially the east tropical Atlantic (Figures 6a, 6b, 7a, and 7b). The Atlantic warm pool during the AMO positive phase reduces low-level easterlies and upper westerlies, and thus weakens the vertical wind shear (Kossin & Vimont, 2007; C. Wang et al., 2008; R. Zhang & Delworth, 2006). An abnormal low-level cyclone over the African coast (Figure 8b) induced by tropical Atlantic SST warming brings moisture to the NA, increasing the relative humidity (Hagos & Cook, 2008; Wu et al., 2010). Additionally, the PDO negative phase can motivate a Gill-type Rossby wave response over the tropical Pacific and Atlantic, intensify westerlies to the east tropical Atlantic, and then trigger an abnormal low-level cyclone over the African coast. However, this Gill-type Rossby wave response has weakened in the last two decades (H. Zhao et al., 2018; J. Zhao et al., 2018), resulting in a weak correlation between the PDO and translation distance of NA TCs. An anomalous anticyclonic steering flow over the northwestern NA guides the TCs generated over the east tropical Atlantic northwestward to the North American mainland, resulting in relatively longer TC tracks.

3.3. Synergetic Influences of PDO and AMO Phase Shifts on TC Translation Distance

The basins with significant correlations between TC translation distance and both PDO and AMO are those in the Pacific, that is, WNP, ENP, and SP; and, positive (negative) correlations with PDO (AMO) occurs in all the three basins. This suggests that the phase shifts of PDO and AMO may enhance their individual influences on translation distance of TCs over the Pacific at a multidecadal timescale. Based on the composited results of SST, GPI, potential intensity, vertical wind shear, low-level relative humidity, steering flow, and 500-hPa zonal wind (Figures 4–8; Figure S9 in Supporting Information S1), we propose a schematic diagram of synergetic influences of PDO and AMO phase shifts on TC translation distance in the Pacific (Figure 9).

Inter-ocean interactions can initiate and/or modulate global TC activities by exerting a remote forcing (Sun et al., 2017; C. Wang, 2019; J. Yu et al., 2016). This teleconnection process occurs through either an atmospheric bridge or the global oceanic-wave adjustment. PDO directly affects TC translation distance over the Pacific by altering local SST patterns and modulates the NA TC translation distance through the Atlantic-Pacific Walker circulation (W. Li et al., 2015; C. Wang, 2019; H. Zhao et al., 2018; J. Zhao et al., 2018). Increasing zonal gradient of SST between tropical eastern Pacific and Atlantic during the PDO negative phase and AMO positive phase can strengthen the Atlantic-Pacific Walker circulation featured as intensified westerlies to the east of cooling, and lead to an anomalous cyclonic steering flow over the subtropical Atlantic. And the cyclonic steering flow can provide proper conditions to TC geneses eastward, resulting in relatively longer NA TC tracks in the recent epoch.

AMO may exert a remote forcing on the Indo-Pacific on a multidecadal timescale with two pathways relaying Atlantic signals (Gao et al., 2018; Ham et al., 2013; Rong et al., 2010; J. Yu et al., 2016). The first pathway is an eastward relay of the AMO warm signal to the Pacific (Figure 9a). Warm SST anomalies in the tropical Atlantic during the AMO positive phase initiate a local positive heating, and produce low-level easterly anomalies over the NIO through Gill-type Kelvin wave propagation (Gao et al., 2018; Gill, 1980; Ham et al., 2013). Given pronounced climatological trade westerlies over the NIO in boreal summer, the anomalous easterlies indicate weakened local surface wind speed, which can induce decreased evaporation over the NIO and then warm the local SST. The warm SST anomalies in the NIO further induce anomalous easterlies in the east, leading to an anticyclone over the tropical western Pacific, which generates a cyclonic steering flow over the southwest WNP and then results in shorter cyclogenesis-to-land distance and more frequent landfall of WNP TCs.

The second pathway is a westward relay of the AMO warm signal to the Pacific (Figure 9b; Gao et al., 2018; Ham et al., 2013). Sun et al. (2017) highlighted that the atmospheric teleconnection between the AMO and warm SST anomalies in the tropical Atlantic and the North Pacific weakens the Aleutian low and enhances the subtropical North Pacific easterlies, inducing subtropical WNP SST warming through a wind–evaporation–SST effect. The increasing zonal gradient of SST between the tropical eastern Pacific and Atlantic in the last two decades can strengthen the Atlantic-Pacific Walker circulation (Figure 9b). It is featured as westerlies in the tropic ENP and easterlies in the subtropics ENP as a Gill-type Rossby wave response (Gill, 1980). This response can enhance the cyclonic steering flow over the southeast ENP and westerlies in the tropic ENP, which promotes ENP TC genesis landward. The strengthened Atlantic-Pacific Walker circulation can also enhance vertical wind shear and anticyclonic steering flow over the tropical western Pacific, suppressing WNP TC genesis away from the mainland (W. Zhang et al., 2018).

The Atlantic-Pacific Walker circulation strengthened by warm SST anomalies during the AMO positive phase also affects the Hadley circulation (see the paired cyclone and anticyclone in each basin of the Pacific). The

10.1029/2022EF003079

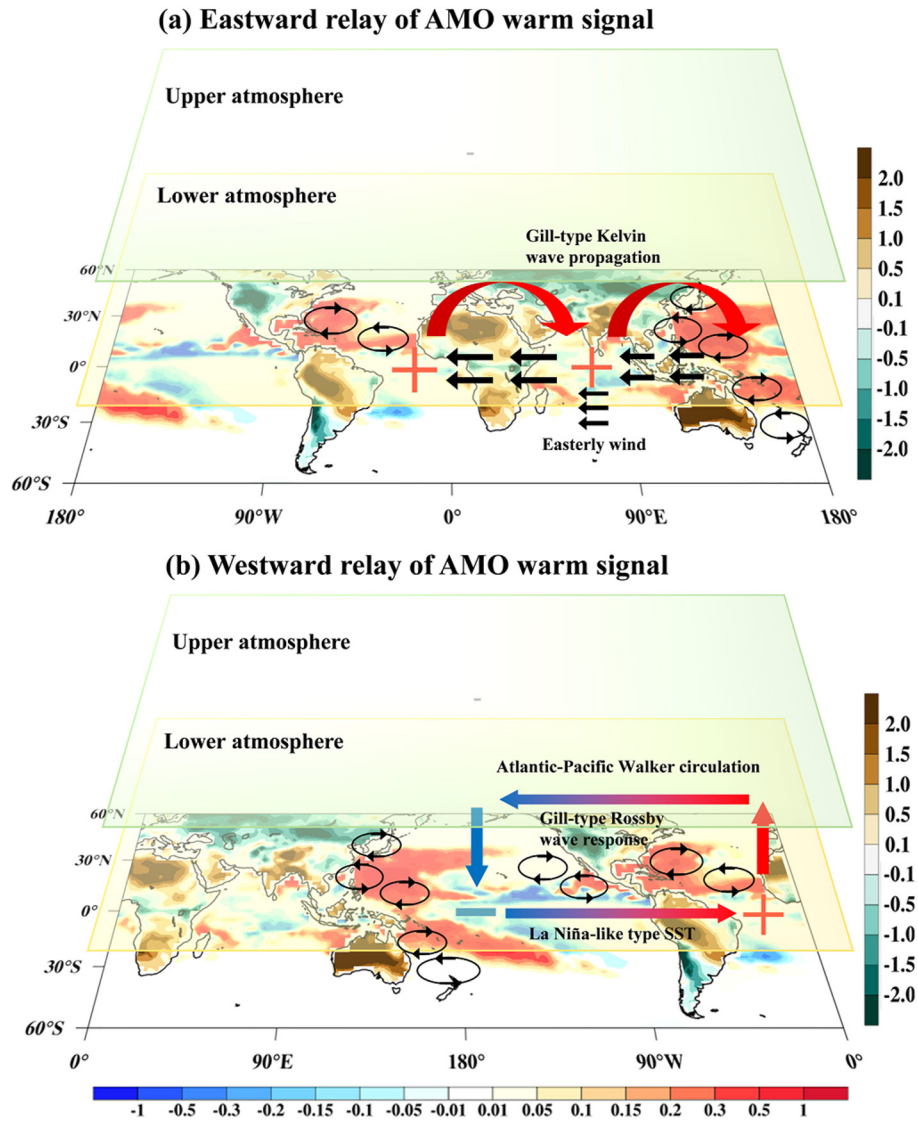

Figure 9. Schematic diagram of Atlantic Multidecadal Oscillation (AMO) warm sea surface temperatures patterns remotely impacting on the Pacific TC translation distance via two pathways: the Indian Ocean (a) and subtropic eastern Pacific (b) relaying effects. The anomalies shown in horizontal (straight) color bar in marine (terrestrial) areas indicate genesis potential index (700-hPa relative humidity; units: %), computed as the absolute difference of TC-season means between the AMO warm phase period (1998–2020) and the reference period 1981–2010. The TC season is July–October (December–March) in the Northern (Southern) Hemisphere. Solid black circles with arrows denote steering flow anomalies. Broad red (blue) arrows denote the Walker circulation ascending (descending) branches. Plus and minus markers denote warm and cold sea surface temperature anomalies, respectively.

anomalous sinking and rising motions associated with the meridionally expanding Hadley circulation are responsible for the poleward migration of Pacific TCs (Sharmila & Walsh, 2018). The zonal migration of Pacific TCs is dominated by the Walker circulation (S. S. Wang & Toumi, 2021). H. Zhao et al. (2019) indicated that the co-variability of TC genesis longitude and latitude in the WNP during 1998–2016 is caused by the intensity of both the Hadley and Walker circulations. Further work is needed to investigate the coupled mechanisms of the Hadley and Walker circulations in terms of their impact the on Pacific TC translation distance.

4. Conclusions

Based on the IBTrACS TC best track data set and ERA5 reanalysis data, we investigated long-term changes in translation distance of global TCs during 1975–2020, and explored the relationship of these changes with the

PDO and AMO. Long-term decreasing trends in the translation distance of all and landfalling TCs are found over the globe, Northern Hemisphere, and Southern Hemisphere. However, these decreasing trends are not monotonous but step-like. Specifically, an abrupt change point around the year 1997 in the time series of annual-mean TC translation distance marks a shift from increasing trends during 1975–1997 to decreasing trends during 1998–2020 (and from higher to lower TC translation distance on average). This change point is equally evident for landfall and non-landfalling TCs, and for over-land and over-sea translation distance of landfalling TCs. It is noted that the decrease in mean TC translation distance is sharper for landfalling TCs than non-landfalling TCs, and for over-land than over-sea landfalling TCs. We find that the observed drop (sudden increase) in the distance between TC genesis locations and land (the percentage of landfalling TCs) is highly consistent with the drop in TC translation distance. The decrease in distance to land, and the sudden increase in the percentage of landfalling TCs are both directly responsible for the shift in TC translation distance.

Both the PDO and AMO shift their phases in the mid-1990s. These phase shifts are consistent with the abrupt change point in TC translation distance, implying that the PDO and AMO are likely to be the potential drivers. The significant correlations between TC translation distance and the PDO and AMO indices confirm that phase shifts of the PDO and AMO are associated with the decadal changes in the translation distance of TCs, especially over the Pacific. The last 20 years have mainly experienced PDO negative and AMO positive phases, which lead to an enhanced GPI and potential intensity in the offshore areas of the six global TC basins, and thus global TC landward genesis. Additionally, changes in environmental patterns (vertical wind shear, low-level relative humidity, and steering flow) driven by the PDO and AMO individually and jointly, also appear to play important roles in the step-like decrease in the translation distance of TCs, especially in the Pacific. The La Niña-like SST anomalies during the PDO negative phase induce weakened vertical wind shear and increased low-level relative humidity over the subtropical WNP, ENP offshore areas, and southwest SP, providing favorable thermodynamic and dynamic conditions for the TC genesis in the Pacific, both poleward and landward. The dominant westward steering flow over the Pacific also plays an important role in the decrease in Pacific TC translation distance. These changes in circulation patterns in the Pacific are enhanced by the remote warm SST anomalies in the tropical Atlantic via two pathways: the Indian Ocean and subtropical eastern Pacific relaying effects.

Our study is the first to reveal decadal changes in global TC translation distance, which are consistent with the decadal changes in TC frequency. We further find significant correlations between the decadal change in TC translation distance and PDO and AMO, and discuss the potential mechanisms explaining how the PDO and AMO phase switch may modulate the changes in the translation distance of TCs, especially over the Pacific. We acknowledge that this discussion is primary and largely observational, and further modeling evidence is required. Nevertheless, our work provides a direction for the future works, and suggests that the PDO and AMO are potential drivers that may be used to improve the predictability of decadal changes in TC translation distance, especially over the Pacific.

Data Availability Statement

Tropical cyclone track data from the International Best Track Archive for Climate Stewardship is available at https://doi.org/10.25921/82ty-9e16. Monthly PDO and AMO indices are available at https://psl.noaa.gov/gcos_wgsp/Timeseries/PDO/ and https://psl.noaa.gov/data/timeseries/AMO/, respectively. The ERA5 reanalysis data are available at https://www.ecmwf.int/en/forecasts/datasets/reanalysis-datasets/era5.

Acknowledgments
This study is supported by the National Key Research and Development Program of China (Grant 2018YFA0605603), the National Natural Science Foundation of China (Grant U1911205, 41901041, and 42001042), the Pre-research Project of SongShan Laboratory (No. YYYY062022001), and the Guiding project of Scientific Research Plan of Education Department of Hubei Province (Grant B2022265). X. Gu is supported by the China Scholarship Council.

References

Allen, R. J., & Kovilakam, M. (2017). The role of natural climate variability in recent tropical expansion. *Journal of Climate*, *30*(16), 6329–6350. https://doi.org/10.1175/JCLI-D-16-0735.1

Altman, J., Ukhvatkina, O. N., Omelko, A. M., Macek, M., Plener, T., Pejcha, V., et al. (2018). Poleward migration of the destructive effects of tropical cyclones during the 20th century. *Proceedings of the National Academy of Sciences of the United States of America*, *115*(45), 11543–11548. https://doi.org/10.1073/pnas.1808979115

Aryal, Y. N., Villarini, G., Zhang, W., & Vecchi, G. A. (2018). Long term changes in flooding and heavy rainfall associated with North Atlantic tropical cyclones: Roles of the North Atlantic Oscillation and El Niño-Southern Oscillation. *Journal of Hydrology*, *559*, 698–710. https://doi.org/10.1016/j.jhydrol.2018.02.072

Camargo, S. J., Emanuel, K. A., & Sobel, A. H. (2007). Use of a genesis potential index to diagnose ENSO effects on tropical cyclone genesis. *Journal of Climate*, *20*(19), 4819–4834. https://doi.org/10.1175/JCLI4282.1

Camargo, S. J., Sobel, A. H., Barnston, A. G., & Emanuel, K. A. (2007). Tropical cyclone genesis potential index in climate models. *Tellus A*, *59*(4), 428–443. https://doi.org/10.1111/j.1600-0870.2007.00238.x

Cao, J., Zhao, H., Wang, B., & Wu, L. (2021). Hemisphere-asymmetric tropical cyclones response to anthropogenic aerosol forcing. *Nature Communications*, *12*(1), 6787. https://doi.org/10.1038/s41467-021-27030-z

Chan, K. T. F. (2019). Are global tropical cyclones moving slower in a warming climate? *Environmental Research Letters*, *14*(10), 104015. https://doi.org/10.1088/1748-9326/ab4031

Chen, J., Tam, C.-Y., Cheung, K., Wang, Z., Murakami, H., Lau, N.-C., et al. (2021). Changing impacts of tropical cyclones on east and southeast Asian inland regions in the past and a globally warmed future climate. *Frontiers of Earth Science*, *9*. https://doi.org/10.3389/feart.2021.769005

Chen, X., Wu, L., & Zhang, J. (2011). Increasing duration of tropical cyclones over China. *Geophysical Research Letters*, *38*(2), L02708. https://doi.org/10.1029/2010GL046137

Cheung, K. K. W., Jiang, N., Liu, K. S., & Chang, L. T. C. (2015). Interdecadal shift of intense tropical cyclone activity in the Southern Hemisphere. *International Journal of Climatology*, *35*(7), 1519–1533. https://doi.org/10.1002/joc.4073

Choi, J.-W., & Kim, H.-D. (2019). Negative relationship between Korea landfalling tropical cyclone activity and Pacific Decadal Oscillation. *Dynamics of Atmospheres and Oceans*, *87*, 101100. https://doi.org/10.1016/j.dynatmoce.2019.101100

Cui, J., Piao, S., Huntingford, C., Wang, X., Lian, X., Chevuturi, A., et al. (2020). Vegetation forcing modulates global land monsoon and water resources in a CO_2-enriched climate. *Nature Communications*, *11*(1), 1–11. https://doi.org/10.1038/s41467-020-18992-7

Czajkowski, J., Villarini, G., Michel-Kerjan, E., & Smith, J. A. (2013). Determining tropical cyclone inland flooding loss on a large scale through a new flood peak ratio-based methodology. *Environmental Research Letters*, *8*(4), 044056. https://doi.org/10.1088/1748-9326/8/4/044056

Dai, Y., Wang, B., & Sun, W. (2022). What drives the decadal variability of global tropical storm days from 1965 to 2019? *Advances in Atmospheric Sciences*, *39*(2), 344–353. https://doi.org/10.1007/s00376-021-0354-1

Daloz, A. S., & Camargo, S. J. (2018). Is the poleward migration of tropical cyclone maximum intensity associated with a poleward migration of tropical cyclone genesis? *Climate Dynamics*, *50*(1–2), 705–715. https://doi.org/10.1007/s00382-017-3636-7

Emanuel, K. A. (2005). Increasing destructiveness of tropical cyclones over the past 30 years. *Nature*, *436*(7051), 686–688. https://doi.org/10.1038/nature03906

Emanuel, K. A. (2007). Environmental factors affecting tropical cyclone power dissipation. *Journal of Climate*, *20*(22), 5497–5509. https://doi.org/10.1175/1520-0469(2004)061<0843:ECOTCI>2.0.CO;2

Franklin, J. L., Feuer, S. E., Kaplan, J., & Aberson, S. D. (1996). Tropical cyclone motion and surrounding flow relationships: Searching for beta gyres in omega dropwindsonde datasets. *Monthly Weather Review*, *124*(1), 64–84. https://doi.org/10.1175/1520-0493(1996)124<0064:TCMASF>2.0.CO;2

Gao, S., Chen, Z., & Zhang, W. (2018). Impacts of tropical North Atlantic SST on western North Pacific landfalling tropical cyclones. *Journal of Climate*, *31*(2), 853–862. https://doi.org/10.1175/JCLI-D-17-0325.1

Gill, A. E. (1980). Some simple solutions for heat-induced tropical circulation. *Quarterly Journal of the Royal Meteorological Society*, *106*(449), 447–462. https://doi.org/10.1002/qj.49710644905

Hagos, S. M., & Cook, K. H. (2008). Ocean warming and Late-Twentieth-Century Sahel drought and recovery. *Journal of Climate*, *21*(15), 3797–3814. https://doi.org/10.1175/2008JCLI2055.1

Ham, Y. G., Kug, J. S., Park, J. Y., & Jin, F. F. (2013). Sea surface temperature in the north tropical Atlantic as a trigger for El Niño/Southern Oscillation events. *Nature Geoscience*, *6*(2), 112–116. https://doi.org/10.1038/ngeo1686

Han, W., Vialard, J., McPhaden, M. J., Lee, T., Masumoto, Y., Feng, M., & De Ruijter, W. P. M. (2014). Indian ocean decadal variability: A review. *Bulletin of the American Meteorological Society*, *95*(11), 1679–1703. https://doi.org/10.1175/BAMS-D-13-00028.1

He, H., Yang, J., Gong, D., Mao, R., Wang, Y., & Gao, M. (2015). Decadal changes in tropical cyclone activity over the western North Pacific in the late 1990s. *Climate Dynamics*, *45*(11–12), 3317–3329. https://doi.org/10.1007/s00382-015-2541-1

Hersbach, H., Bell, B., Berrisford, P., Hirahara, S., Horányi, A., Muñoz-Sabater, J., et al. (2020). The ERA5 global reanalysis. *Quarterly Journal of the Royal Meteorological Society*, *146*(730), 1999–2049. https://doi.org/10.1002/qj.3803

Holland, G. J. (2007). Misuse of landfall as a proxy for Atlantic tropical cyclone activity. *Eos, Transactions American Geophysical Union*, *88*(36), 349–350. https://doi.org/10.1029/2007EO360001

Hsu, P. C., Chu, P. S., Murakami, H., & Zhao, X. (2014). An abrupt decrease in the late-season typhoon activity over the western North Pacific. *Journal of Climate*, *27*(11), 4296–4312. https://doi.org/10.1175/JCLI-D-13-00417.1

Kerry, E. (2020). Evidence that hurricanes are getting stronger. *Proceedings of the National Academy of Sciences of the United States of America*, *117*(24), 13194–13195. https://doi.org/10.1073/pnas.2007742117

Knapp, K. R., Kruk, M. C., Levinson, D. H., Diamond, H. J., & Neumann, C. J. (2010). The international best track archive for climate stewardship (IBTrACS) unifying tropical cyclone data. *Bulletin of the American Meteorological Society*, *91*(3), 363–376. https://doi.org/10.1175/2009BAMS2755.1

Knutson, T., Camargo, S. J., Chan, J. C. L., Emanuel, K., Ho, C. H., Kossin, J., et al. (2020). Tropical cyclones and climate change assessment: Part II: Projected response to anthropogenic warming. *Bulletin of the American Meterological Society*, *101*(3), E303–E322. https://doi.org/10.1175/BAMS-D-18-0194.1

Knutson, T. R., McBride, J. L., Chan, J., Emanuel, K., Holland, G., Landsea, C., et al. (2010). Tropical cyclones and climate change. *Nature Geoscience*, *3*(3), 157–163. https://doi.org/10.1038/ngeo779

Kossin, J. P. (2018). A global slowdown of tropical-cyclone translation speed. *Nature*, *558*(7708), 104–107. https://doi.org/10.1038/s41586-018-0158-3

Kossin, J. P., Emanuel, K. A., & Vecchi, G. A. (2014). The poleward migration of the location of tropical cyclone maximum intensity. *Nature*, *509*(7500), 349–352. https://doi.org/10.1038/nature13278

Kossin, J. P., Knapp, K. R., Olander, T. L., & Vekden, C. S. (2020). Global increase in major tropical cyclone exceedance probability over the past four decades. *Proceedings of the National Academy of Sciences of the United States of America*, *117*(22), 11975–11980. https://doi.org/10.1073/pnas.1920849117

Kossin, J. P., & Vimont, D. J. (2007). A more general framework for understanding Atlantic hurricane variability and trends. *Bulletin of the American Meteorological Society*, *88*(11), 1767–1782. https://doi.org/10.1175/BAMS-88-11-1767

Lai, Y., Li, J., Gu, X., Chen, Y., Kong, D., Gan, T., et al. (2020). Greater flood risks in response to slowdown of tropical cyclones over the coast of China. *Proceedings of the National Academy of Sciences of the United States of America*, *117*(26), 14751–14755. https://doi.org/10.1073/pnas.1918987117

Lai, Y., Li, J., Gu, X., Liu, C., & Chen, Y. (2021). Global compound floods from precipitation and storm surge: Hazards and the roles of cyclones. *Journal of Climate*, *34*(20), 8319–8339. https://doi.org/10.1175/JCLI-D-21-0050.1

Lanzante, J. R. (2019). Uncertainties in tropical-cyclone translation speed. *Nature*, *570*(7759), E6–E15. https://doi.org/10.1038/s41586-019-1223-2

Lee, T.-C., Knutson, T. R., Nakaegawa, T., Ying, M., & Cha, E. J. (2020). Third assessment on impacts of climate change on tropical cyclones in the typhoon committee region—Part I: Observed changes, detection and attribution. *Tropical Cyclone Research and Review*, *9*(1), 1–22. https://doi.org/10.1016/j.tcrr.2020.03.001

Li, C., Gu, X., Slater, L. J., Liu, J., Li, J., Zhang, X., & Kong, D. (2023). Urbanization-induced increases in heavy precipitation are magnified by moist heatwaves in an urban agglomeration of East China. *Journal of Climate*, *36*(2), 693–709. https://doi.org/10.1175/JCLI-D-22-0223.1

Li, L., & Chakraborty, P. (2020). Slower decay of landfalling hurricanes in a warming world. *Nature*, *587*(7833), 230–234. https://doi.org/10.1038/s41586-020-2867-7

Li, W., Li, L., & Deng, Y. (2015). Impact of the interdecadal Pacific oscillation on tropical cyclone activity in the North Atlantic and eastern North Pacific. *Scientific Reports*, *5*(1), 12358. https://doi.org/10.1038/srep12358

Liu, J., You, Y., Li, J., Sitch, S., Gu, X., Nabel, J. E. M. S., et al. (2021). Response of global land evapotranspiration to climate change, elevated CO_2, and land use change. *Agricultural and Forest Meteorology*, *311*, 108663. https://doi.org/10.1016/j.agrformet.2021.108663

Moon, I.-J., Kim, S.-H., & Chan, J. C. L. (2019). Climate change and tropical cyclone trend. *Nature*, *570*(7759), E3–E5. https://doi.org/10.1038/s41586-019-1222-3

Murakami, H. (2022). Substantial global influence of anthropogenic aerosols on tropical cyclones over the past 40 years. *Science Advances*, *8*(19), eabn9493. https://doi.org/10.1126/sciadv.abn9493

Murakami, H., Delworth, T. L., Cooke, W. F., Zhao, M., Xiang, B., & Hsu, P.-C. (2020). Detected climatic change in global distribution of tropical cyclones. *Proceedings of the National Academy of Sciences of the United States of America*, *117*(20), 10706–10714. https://doi.org/10.1073/pnas.1922500117

Murakami, H., Vecchi, G. A., & Underwood, S. (2017). Increasing frequency of extremely severe cyclonic storms over the Arabian Sea. *Nature Climate Change*, *7*(12), 885–889. https://doi.org/10.1038/s41558-017-0008-6

Patricola, C. M., & Wehner, M. F. (2018). Anthropogenic influences on major tropical cyclone events. *Nature*, *563*(7731), 339–346. https://doi.org/10.1038/s41586-018-0673-2

Pettitt, A. N. (1979). A non-parametric approach to the change-point problem. *Journal of the Royal Statistical Society. Series C (Applied Statistics)*, *28*(2), 126–135. https://doi.org/10.2307/2346729

Pielke, R. A., Landsea, C., Mayfield, M., Layer, J., & Pasch, R. (2005). Hurricanes and global warming. *Bulletin of the American Meteorological Society*, *86*(11), 1571–1576. https://doi.org/10.1175/BAMS-86-11-1571

Rong, X., Zhang, R., & Li, T. (2010). Impacts of Atlantic sea surface temperature anomalies on Indo-East Asian summer monsoon-ENSO relationship. *Chinese Science Bulletin*, *55*(22), 2458–2468. https://doi.org/10.1007/s11434-010-3098-3

Scoccimarro, E., Gualdi, S., Bellucci, A., Peano, D., Cherchi, A., Vecchi, G. A., & Navarra, A. (2020). The typhoon-induced drying of the Maritime Continent. *Proceedings of the National Academy of Sciences of the United States of America*, *117*(8), 3983–3988. https://doi.org/10.1073/pnas.1915364117

Scoccimarro, E., Villarini, G., Gualdi, S., & Navarra, A. (2021). The Pacific Decadal Oscillation modulates tropical cyclone days on the interannual timescale in the North Pacific Ocean. *Journal of Geophysical Research: Atmospheres*, *126*(15), e2021JD034988. https://doi.org/10.1029/2021JD034988

Shan, K., & Yu, X. (2020). Enhanced understanding of poleward migration of tropical cyclone genesis. *Environmental Research Letters*, *15*(10), 104062. https://doi.org/10.1088/1748-9326/abaf85

Sharmila, S., & Walsh, K. J. E. (2018). Recent poleward shift of tropical cyclone formation linked to Hadley cell expansion. *Nature Climate Change*, *8*(8), 730–736. https://doi.org/10.1038/s41558-018-0227-5

Shi, D., Ge, X., Peng, M., & Li, T. (2020). Characterization of tropical cyclone rapid intensification under two types of El Niño events in the western North Pacific. *International Journal of Climatology*, *40*(4), 2359–2372. https://doi.org/10.1002/joc.6338

Simpson, R. H., & Riehl, H. (1981). *The hurricane and its impact*. Louisiana State University Press. https://doi.org/10.2307/633363

Sobel, A. H., Camargo, S. J., Hall, T. M., Lee, C. Y., Tippett, M. K., & Wing, A. A. (2016). Human influence on tropical cyclone intensity. *Science*, *353*(6296), 242–246. https://doi.org/10.1126/science.aaf6574

Staten, P. W., Lu, J., Grise, K. M., Davis, S. M., & Birner, T. (2018). Re-examining tropical expansion. *Nature Climate Change*, *8*(9), 768–775. https://doi.org/10.1038/s41558-018-0246-2

Studholme, J., Fedorov, A. V., Gulev, S. K., Emanuel, K., & Hodges, K. (2022). Poleward expansion of tropical cyclone latitudes in warming climates. *Nature Geoscience*, *15*(1), 14–28. https://doi.org/10.1038/s41561-021-00859-1

Sun, C., Kucharski, F., Li, J., Jin, F., Kang, I., & Ding, R. (2017). Western tropical Pacific multidecadal variability forced by the Atlantic multidecadal oscillation. *Nature Communications*, *8*(1), 1–10. https://doi.org/10.1038/ncomms15998

Villarini, G., Goska, R., Smith, J. A., & Vecchi, G. A. (2014). North Atlantic tropical cyclones and U.S. flooding. *Bulletin of the American Meteorological Society*, *95*(9), 1381–1388. https://doi.org/10.1175/BAMS-D-13-00060.1

Wang, C. (2019). Three-ocean interactions and climate variability: A review and perspective. *Climate Dynamics*, *53*(7–8), 5119–5136. https://doi.org/10.1007/s00382-019-04930-x

Wang, C., Lee, S.-K., & Enfield, D. B. (2008). Atlantic warm pool acting as a link between Atlantic multidecadal oscillation and Atlantic tropical cyclone activity. *Geochemistry, Geophysics, Geosystems*, *9*(5), Q05V03. https://doi.org/10.1029/2007GC001809

Wang, L., Gu, X., Gulakhmadov, A., Li, J., Slater, L. J., Zhang, Q., et al. (2022). An analysis of translation distance of tropical cyclones over the western North Pacific. *Journal of Climate*, *35*(23), 4043–4060. https://doi.org/10.1175/JCLI-D-22-0030.1

Wang, L., Yang, Z., Gu, X., & Li, J. (2020). Linkages between tropical cyclones and extreme precipitation over China and the role of ENSO. *International Journal of Disaster Risk Science*, *11*(4), 538–553. https://doi.org/10.1007/s13753-020-00285-8

Wang, R., & Wu, L. (2013). Climate changes of Atlantic tropical cyclone formation derived from Twentieth-Century Reanalysis. *Journal of Climate*, *26*(22), 8995–9005. https://doi.org/10.1175/JCLI-D-13-00056.1

Wang, S., & Toumi, R. (2021). Recent migration of tropical cyclones toward coasts. *Science*, *371*(6528), 514–517. https://doi.org/10.1126/science.abb9038

Wang, X., Wang, C., Zhang, L., & Wang, X. (2015). Multidecadal variability of tropical cyclone rapid intensification in the western North Pacific. *Journal of Climate*, *28*(9), 3806–3820. https://doi.org/10.1175/JCLI-D-14-00400.1

Wei, L., Gu, X., Kong, D., & Liu, J. (2021). A long-term perspective of hydroclimatological impacts of tropical cyclones on regional heavy precipitation over eastern monsoon China. *Atmospheric Research*, *264*, 105862. https://doi.org/10.1016/j.atmosres.2021.105862

Wu, L., Tao, L., & Ding, Q. (2010). Influence of sea surface warming on environmental factors affecting long-term changes of Atlantic tropical cyclone formation. *Journal of Climate*, *23*(22), 5978–5989. https://doi.org/10.1175/2010JCLI3384.1

Wu, L., & Wang, B. (2008). What has changed the proportion of intense hurricanes in the last 30 years? *Journal of Climate*, *21*(6), 1432–1439. https://doi.org/10.1175/2007JCLI1715.1

Yong, L., & Chen, D. (2019). An interdecadal change in the interannual variability of boreal summer tropical cyclone genesis frequency over the western North Pacific around the early 1990s. *Theoretical and Applied Climatology*, *137*(3), 1843–1853. https://doi.org/10.1007/s00704-018-2710-3

Yu, J., Li, T., Tan, Z., & Zhu, Z. (2016). Effects of tropical North Atlantic SST on tropical cyclone genesis in the western North Pacific. *Climate Dynamics*, *46*(3–4), 865–877. https://doi.org/10.1007/s00382-015-2618-x

Yu, X., Gu, X., Kong, D., Zhang, Q., Cao, Q., Slater, L. J., et al. (2022). Asymmetrical shift toward less light and more heavy precipitation in an urban agglomeration of east China: Intensification by erbanization. *Geophysical Research Letters*, *49*(4), e2021GL097046. https://doi.org/10.1029/2021GL097046

Zehr, R. M. (2003). Environmental vertical wind shear with Hurricane Bertha (1996). *Weather and Forecasting*, *18*(2), 345–356. https://doi.org/10.1175/1520-0434(2003)018<0345:EVWSWH>2.0.CO;2

Zhang, G., Murakami, H., Knutson, T. R., Mizuta, R., & Yoshida, K. (2020). Tropical cyclone motion in a changing climate. *Science Advances*, *6*(17). https://doi.org/10.1126/sciadv.aaz7610

Zhang, Q., Gu, X., Li, J., Shi, P., & Singh, V. P. (2018). The impact of tropical cyclones on extreme precipitation over coastal and inland areas of China and its association to ENSO. *Journal of Climate*, *31*(5), 1865–1880. https://doi.org/10.1175/JCLI-D-17-0474.1

Zhang, Q., Gu, X., Shi, P., & Singh, V. P. (2017). Impact of tropical cyclones on flood risk in southeastern China: Spatial patterns, causes and implications. *Global and Planetary Change*, *150*, 81–93. https://doi.org/10.1016/j.gloplacha.2017.02.004

Zhang, R., & Delworth, T. L. (2006). Impact of Atlantic multidecadal oscillations on India/Sahel rainfall and Atlantic hurricanes. *Geophysical Research Letters*, *33*(17), L17712. https://doi.org/10.1029/2006GL026267

Zhang, W., Vecchi, G. A., Murakami, H., Villarini, G., Delworth, T. L., Yang, X., & Jia, L. (2018). Dominant role of Atlantic multidecadal oscillation in the recent decadal changes in western North Pacific tropical cyclone activity. *Geophysical Research Letters*, *45*(1), 354–362. https://doi.org/10.1002/2017GL076397

Zhang, Z., Sun, X., & Yang, X. Q. (2018). Understanding the interdecadal variability of East Asian summer monsoon precipitation: Joint influence of three oceanic signals. *Journal of Climate*, *31*(14), 5485–5506. https://doi.org/10.1175/JCLI-D-17-0657.1

Zhao, H., Duan, X., Raga, G. B., & Sun, F. (2018). Potential large-scale forcing mechanisms driving enhanced North Atlantic tropical cyclone activity since the mid-1990s. *Journal of Climate*, *31*(4), 1377–1397. https://doi.org/10.1175/JCLI-D-17-0016.1

Zhao, H., Zhang, J., Klotzbach, P. J., & Chen, S. (2019). Recent increased covariability of tropical cyclogenesis latitude and longitude over the western North Pacific during the extended boreal summer. *Journal of Climate*, *32*(23), 8167–8179. https://doi.org/10.1175/JCLI-D-19-0009.1

Zhao, J., Zhan, R., Wang, Y., & Xu, H. (2018). Contribution of the interdecadal Pacific oscillation to the recent abrupt decrease in tropical cyclone genesis frequency over the western North Pacific since 1998. *Journal of Climate*, *31*(20), 8211–8224. https://doi.org/10.1175/JCLI-D-18-0202.1